IEEE Access
Multidisciplinary | Rapid Review | Open Access Journal

Received May 23, 2019, accepted July 18, 2019, date of publication July 23, 2019, date of current version August 9, 2019.

Digital Object Identifier 10.1109/ACCESS.2019.2930545

Fault Diagnosis of Power Systems Based on Temporal Constrained Fuzzy Petri Nets

BIAO XU[1], XIN YIN[2], (Member, IEEE), XIANGGEN YIN[1], (Member, IEEE), YIKAI WANG[1], AND SHUAI PANG[1]

[1]State Key Laboratory of Advanced Electromagnetic Engineering and Technology, Huazhong University of Science and Technology, Wuhan 430074, China
[2]Department of Electrical Engineering and Electronics, University of Liverpool, Liverpool L69 3GJ, U.K.

Corresponding author: Xianggen Yin (xgyin@hust.edn.cn)

This work was supported in part by the Key Project of Smart Grid Technology and Equipment of National Key Research and Development Plan of China, under Grant 2017YFB0902900.

ABSTRACT Modern power systems are equipped with comprehensive protective devices to remove the fault section, and the fault diagnosis problem is to interpret the alarms of the protective devices and estimate the fault section. To deal with the uncertainty and temporal constraint of the alarms, a novel fault diagnosis model based on the temporal constrained fuzzy Petri nets (TCFPNs) is proposed in this paper. The truth degree and the timing contribute of the alarms are introduced into the graphic model of the TCFPNs, and the matrix algorithm, considering both the fuzzy reasoning and temporal reasoning, is carried out to obtain the fault probability as well as the time point constraint of each candidate section. The developed approach is performed on different test systems for case studies, and the results demonstrate the feasibility, efficiency, and fault tolerance of the method.

INDEX TERMS Power system, fault diagnosis, fuzzy reasoning, temporal constraint, TCFPNs.

I. INTRODUCTION

Morden power systems are equipped with comprehensive protective devices (PDs), such as the cooperated protective relays (PRs) and the circuit breakers (CBs), to remove the fault from the system as soon as possible. This can enhance the selectivity and reliability of fault isolating, but also increase the volume of the alarms, which will pour into the dispatching centre in a short period after the fault. Using these alarms to identify the fault section or sections is the main issue with fault diagnosis. This task can be very hard for dispatchers, especially when the fault scenarios are accompanied with the distortion or loss of the alarms. Therefore, it is critical to develop an effective fault diagnosis system, and provide the dispatcher with processed information in making decisions.

To this end, various kinds of methods have been proposed for power system fault diagnosis, including expert system [1], [2], artificial neural network [3], [4], Bayesian network [5], [6], fuzzy digraph model [7], [8], analytic model [9], [10], and Petri nets [11]–[15]. Although these methods have advantages in some respects, they have their own disadvantages. For example, the expert system has difficulty in establishing and maintaining the knowledge base; the artificial neural network lacks the ability to interpret the reasoning results; the fuzzy rules and membership functions of the fuzzy theory are subject to subjective influences; the prior probability is difficult to obtain for Bayesian network; the analytic model based methods need to be solved iteratively, and the efficiency is not high enough.

The Petri nets based method describes the causality relationship of events by graphic model and achieves rapid reasoning by matrix execution. Therefore, this method has clear physical meaning and strong mathematical foundations, and attracts more and more attention.

The basic discrete Petri nets (DPNs) for power system fault diagnosis are proposed in [11], [12], and the fault section can be identified using the binary action information of the PDs. Enhanced with the fuzzy logic, the fuzzy Petri nets (FPNs) are built to represent a fuzzy production rule-based system in [13], and the execution rules of the model are defined based on the fuzzy reasoning algorithm. Since the FPNs based method has good reasoning advantage compared with the traditional Petri nets, it has been widely used in various fields such as knowledge representation and acquisition [14], reliability analysis [15], and fault diagnosis [16].

In [17], the FPNs are used to estimate the fault section of the power system and the truth degree of the fault section can be obtained through fuzzy reasoning. In [18], the structure

The associate editor coordinating the review of this manuscript and approving it for publication was Yong Fu.

of the FPNs is optimized and the inference algorithm is performed in matrix operation, and these improvements can greatly enhance the adaptability and efficiency of the method. The adaptive fuzzy Petri nets are then proposed in [19], where the weights of the model are dynamically determined by the incomplete and uncertain alarms. Therefore, this model has better learning ability and can adapt to different fault scenarios. In [20], the intuitionistic fuzzy Petri nets are proposed to consider both the certainty and uncertainty of events, and gain better diagnose performance.

The above researches can deal with the uncertainties of the PDs, nevertheless, the timing contributes and the temporal constraints of the alarms are not well considered. With the extensive application of the global positioning system (GPS) clock in substation, a synchronous timestamp can be marked for each alarm by the sequence of events system (SOE). Since the PDs are set to operate with a certain temporal logic, it's of great importance to well employ the temporal information to enhance the fault diagnosis system.

In [21]–[23], the temporal information of alarms is introduced into the expert system, artificial neural network, and analytic model for fault diagnosis respectively, but the effect is not significant for lack of effective temporal reasoning methods. The temporal constraint network (TCN) is a kind of directed acyclic graph suitable for temporal reasoning in the artificial intelligence field [24], and has been introduced into power system fault diagnosis recently. For instance, the TCN is proposed to estimate the fault section of power system in [25] and [26], and the precise timing is not required. In [27], the TCN is applied to describe the temporal constraint between events, and an abductive reasoning based method was developed for power system fault diagnosis. In [28] and [29], the fuzzy Petri nets based model is enhanced with temporal constraints, and the temporal reasoning of TCN is introduced to modify the trust degree of each event, so as to improve accuracy and fault tolerance.

While these existing methods seem appealing to fault section estimation, they still suffer from the following problems in temporal reasoning: 1) the TCN model is constructed for the whole system, and the maintenance of the temporal rules is difficult; 2) the temporal reasoning of the TCN is implemented event-by-event, and the process is complex and time-consuming; 3) the TCN model can hardly adapt to the change of system topology or protection configuration.

In this paper, a novel temporal constrained fuzzy Petri nets (TCFPNs) based method is proposed for power system fault diagnosis, and the following three aspects are the major contributions of this paper.

(1) The definition of the TCFPNs is proposed, where the truth degree and timing contribute of the alarms are introduced into the model, and based on the protection configuration of power system, the structure of the graphic model is optimized to enhance adaptability.

(2) The partitioned matrix based structure description of the TCFPNs is constructed, and the layer-by-layer matrix reasoning algorithm is carried out to obtain the fault probability as well as the time point constraint of each candidate section.

(3) The framework of the TCFPNs based power system fault diagnosis method is established, and the testing results of different systems demonstrate the feasibility, efficiency and fault tolerance of the method.

The remainder of this paper is organized as follows. The definition of the TCFPNs is described in Section II. The graphic modeling of the TCFPNs and the matrix execution algorithm are illustrated in Section III. The framework of the fault diagnosis method is introduced in Section IV. Case studies of the IEEE 14-bus power system and an actual power system in China are presented in Section V and conclusions are drawn in Section VI.

II. TEMPORAL CONSTRAINED FUZZY PETRI NETS (TCFPNs)

A. TEMPORAL CONSTRAINT NETWORK (TCN) AND TEMPORAL REASONING OPERATIONS

To represent temporal logic, there are two typical kinds of temporal objects defined as follows.

1) t is a time point, and a time interval $T(t) = [t^-, t^+]$ is defined as a time-point constraint of t, where t^- and t^+ are the lower and upper bounds of $T(t)$, respectively.

2) $d(t_i, t_j) = t_j - t_i$ is the time-distance from t_i to t_j, and a time interval $D(t_i, t_j) = [\Delta t_{ij}^-, \Delta t_{ij}^+]$ is defined as a constraint of $d(t_i, t_j)$, where Δt_{ij}^- and Δt_{ij}^+ are the lower and upper bounds of $d(t_i, t_j)$, respectively.

Based on these two temporal objects, the mathematical description of the TCN can be defined as a five-tuple $\boldsymbol{G} = \{V, E, T, C_1, C_2\}$, where V represents the set of event vertices, E represents the set of directed edges between vertices, T is the set of the time-points for V, C_1 is the set of the time-point constraints for T, and C_2 is the set of the time-distance constraints between the vertices. The detailed descriptions of the tuples can be found in [25]. Since the temporal objects are defined by intervals, the temporal reasoning operations can be defined by interval algebra as follows.

1) Forward reasoning: if $T(t_i)$ and $D(t_i, t_j)$ are given, then the time-point constraint of t_j can be obtained as

$$T(t_j) = T(t_i) + D(t_i, t_j) = [t_i^- + \Delta t_{ij}^-, t_i^+ + \Delta t_{ij}^+] \quad (1)$$

2) Backward reasoning: if $T(t_j)$ and $D(t_i, t_j)$ are given, then the time-point constraint of t_i can be obtained as

$$T(t_i) = T(t_j) - D(t_i, t_j) = [t_j^- - \Delta t_{ij}^+, t_j^+ - \Delta t_{ij}^-] \quad (2)$$

B. DEFINITION OF TCFPNs

Similar to FPNs, the power system events are represented by the propositions of TCFPNs, and the temporal constraints between the events are represented by the rules of TCFPNs. The mathematical description of TCFPNs is as follows.

$$\boldsymbol{S}_{TCFPNs} = \{\boldsymbol{P}, \boldsymbol{R}, \boldsymbol{I}, \boldsymbol{O}, \boldsymbol{\theta}, \boldsymbol{T}, \boldsymbol{D}\}$$

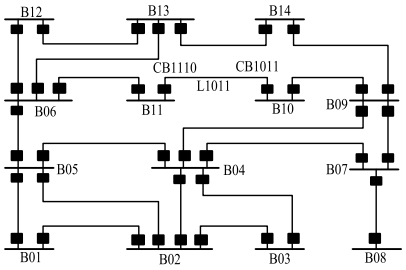

FIGURE 1. The IEEE 14-bus power system.

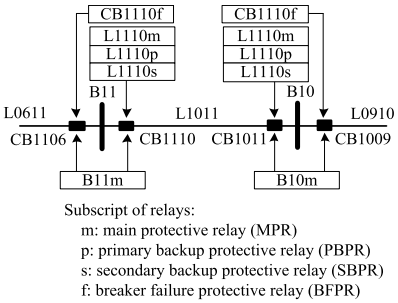

FIGURE 2. The protection configuration of the power system.

where

1) $\boldsymbol{P} = \{p_1, p_2, \ldots, p_m\}$ is a finite set of places or called propositions, where p_i is the i^{th} element of $\boldsymbol{P}$, and identifies the i^{th} event; m is the number of propositions.

2) $\boldsymbol{R} = \{r_1, r_2, \ldots, r_n\}$ is a finite set of transitions or called rules; n is the number of rules.

3) $\boldsymbol{I} = (I_{i,j})_{m\times n}$ is an input matrix defining the directed arcs from propositions to rules. If there is a directed arc from p_i to r_j, then $I_{i,j} = 1$; otherwise, $I_{i,j} = 0$, for $i = 1, 2, \ldots, m$, and $j = 1, 2, \ldots, n$.

4) $\boldsymbol{O} = (O_{i,j})_{m\times n}$ is an output matrix defining the directed arcs from rules to propositions. If there is a directed arc from r_j to p_i, then $O_{i,j} = 1$; otherwise, $O_{i,j} = 0$, for $i = 1, 2, \ldots, m$, and $j = 1, 2, \ldots, n$.

5) $\theta = [\theta_1, \theta_2, \ldots, \theta_m]$ is a truth degree vector, where $\theta_i \in [0, 1]$ means the truth degree of p_i.

6) $\boldsymbol{T} = [T(t_{p1}), T(t_{p2}), \ldots, T(t_{pm})]$ is the set of the time-points mapping to each corresponding element in $\boldsymbol{P}$, the i^{th} element $T(t_{pi})$ represents the time point constraint of the occurrence of p_i.

7) $\boldsymbol{D} = [D(r_1), D(r_2), \ldots, D(r_n)]$ is the set of the time-distance constraints mapping to each corresponding element in $\boldsymbol{R}$, where $D(r_i)$ represents the time-distance constraint between the input and output propositions of r_i.

Compared with the existing FPNs, the main difference is that the time-point constraints and time-distance constraints are introduced for the propositions and rules of the TCFPNs respectively. This is similar with the tuples C_1 and C_2 defined in the TCN. In this way, the fuzzy reasoning and temporal reasoning techniques can be performed together to achieve efficient fault diagnosis. Correspondingly, the operating time point and time delay of the protective devices in the power system can be reflected by the TCFPNs. Therefore, through the reasoning algorithm of TCFPNs, the fault probability as well as the time point constraint of each fault candidate can be obtained simultaneously.

III. POWER SYSTEM FAULT DIAGNOSIS BASED ON TCFPNs

A. TYPICAL PROTECTION CONFIGURATION SCHEME

In this part, the IEEE 14-bus power system shown in Fig. 1 is used to demonstrate the proposed method. The system consists of 34 sections, including 14 buses and 20 transmission lines. To explain the configuration of the protection, a part of the 14-bus power system is taken as an example as shown in Fig. 2. For easy of description, the transmission lines and the PDs are numbered according to the bus. For instance, the transmission line connected with bus B10 and bus B11 are denoted as L1011, and the corresponding circuit breakers are denoted as CB1011 and CB1110 respectively. The detailed operating principle of the protective relays can be found in [28], [29].

Corresponding to the protection configuration, there are four possible schemes in each direction to remove the fault on the transmission line.

1) M-scheme: the main protective relay (MPR) operates and trips off the related CB.

2) F-scheme: the breaker failure protective relay (BFPR) operates and trips off the related CB(s) if the M-scheme fails in fault clearing.

3) P-scheme: the primary backup protective relay (PBPR) operates and trips off the related CB if the M-scheme and F-scheme fail in fault clearing.

4) S-scheme: the secondary backup protective relay (SBPR) installed on the adjacent line operates and trips off the related CB if the M-scheme, F-scheme and P-scheme fail in fault clearing.

Similarly, there are two possible schemes in each direction to clear the fault on the bus.

1) M-scheme: the MPR of the bus operates and trips off the related CB(s).

2) S-scheme: the SBPR of the adjacent line operates and trips off the related CB if the M-scheme fails in fault clearing.

B. GRAPHIC MODELING OF TCFPNs

Similar with the FPNs established in [18], the backward reasoning concept is applied to optimize the structure of the graphic model of TCFPNs, and the model is directly corresponding to the possible fault removal schemes of the section. The difference is that the TCFPNs focus on the causality between the PRs and the CBs, and therefore they are located in different layers of the graphic model. For example, the TCFPNs based diagnosis models of B13 and L1314 are shown in Fig. 3 and Fig. 4.

In Fig. 3, the places $p_1, p_2, \ldots, p_{16}$ represent the event propositions, and the rules $r_1, r_2, \ldots, p_{13}$ represent the trigger relationship between the propositions. The elements in the parentheses represent the time-distance constraints for the

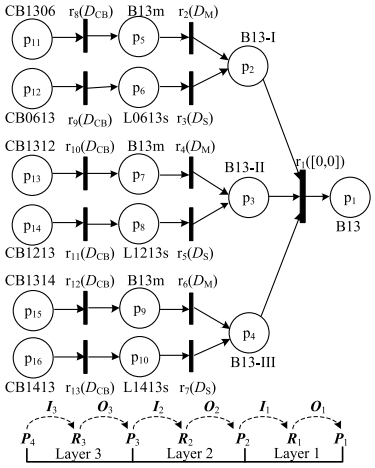

FIGURE 3. The diagnosis model for B13.

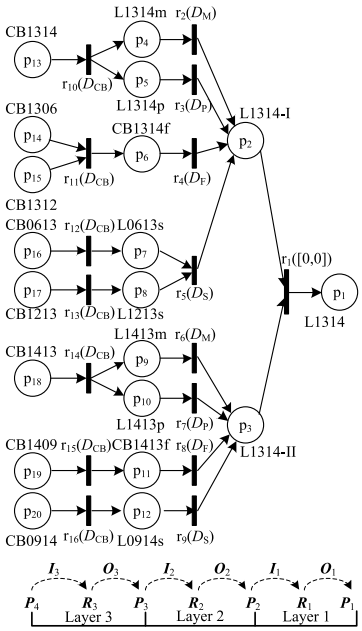

FIGURE 4. The diagnosis model for L1314.

rules (introduced in *Parameter Settings of TCFPNs*). To represent the three outlet directions of B13, the three auxiliary propositions p_2, p_3 and p_4 are introduced into the model, and the time-distance constraint of the intermediate rule r_1 is set to [0, 0].

According to the hierarchical structure of the diagnosis models, the propositions can be grouped as $\boldsymbol{P} = \{\boldsymbol{P}_1, \boldsymbol{P}_2, \boldsymbol{P}_3, \boldsymbol{P}_4\}$, where $\boldsymbol{P}_1$ contains the section proposition, $\boldsymbol{P}_2$ contains the auxiliary propositions, $\boldsymbol{P}_3$ contains the PR propositions, and $\boldsymbol{P}_4$ contains the CB propositions. Similarly, the rules can be grouped as $\boldsymbol{R} = \{\boldsymbol{R}_1, \boldsymbol{R}_2, \boldsymbol{R}_3\}$, and each group represents the trigger relationship between adjacent layers of the model.

Given this background, the input and output matrixes of the TCFPNs can be described in the form of partitioned matrices. For the model shown in Fig. 3, the input and output matrices can be determined and partitioned as Fig. 5.

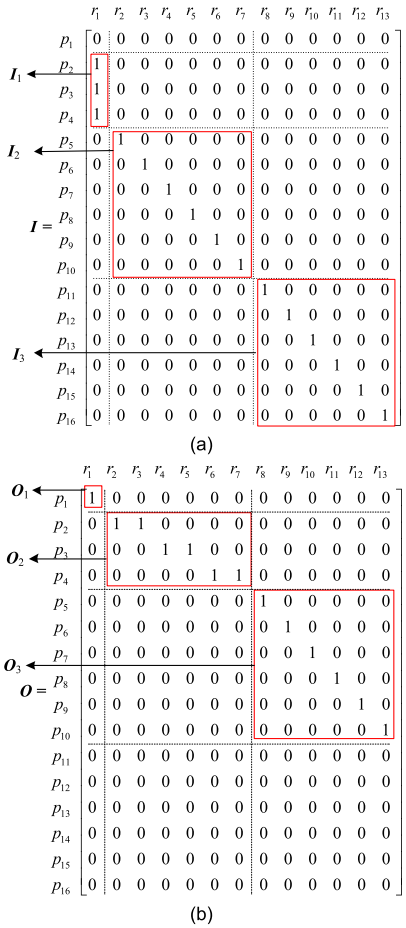

FIGURE 5. The input and output matrices for the diagnosis model of B13. (a) The input matrix. (b) The output matrix.

Obviously, the partitioned matrix description ignores a large number of meaningless zeroes, and the dimension of the matrix operation can be decreased.

C. PARAMETER SETTINGS OF TCFPNs

1) SETTING THE TIME-DISTANCE CONSTRAINT VECTOR *D*

The time-distance constraints for the rules can be set by the time setting values of the protection system. For instance, the PRs are set to operate in a fixed operation delay after the fault, and the corresponding CB is then triggered to trip off with a certain breaking delay. Therefore, the time-distance constraints of the rules in this paper can be determined by considering a certain error based on the time delay, as listed in the Table 1 [28].

2) SETTING THE INITIALIZED TRUTH DEGREE FOR THE PD PROPOSITIONS

Since each proposition of the TCFPNs is associated with a truth degree, the initialized truth degrees for the PD propositions can be specified based on the reliability of the PDs. If the alarm of the PD is actually received, a higher truth degree will be assigned to the proposition. Otherwise, a lower truth degree value will be assigned to the proposition.

TABLE 1. Settings for the time-distance constraint of the rules and the truth degrees of the PD propositions.

Related PDs	Time-distance constraint for the rules (ms)	Initialized truth degree for the propositions	
		Received alarm	Not received alarm
MPR	D_{M}= [10, 20]	0.95	0.4 (for bus) 0.2 (for line)
BFPR	D_{F}= [180, 220]	0.85	0.2
PBPR	D_{P}= [450, 550]	0.8	0.2
SBPR	D_{S}= [1900, 2100]	0.75	0.2
CB	D_{CB}=[40, 60]	0.9	0.2

The initialized truth degrees for the PD propositions are listed in Table 1. Considering that the MPR for the bus are decomposed into many propositions according to the outlet direction, the missing of MPR alarm has a greater impact on the diagnosis result. Therefore, the truth degree for the non-received MPR alarm of bus is set to be 0.4 to guarantee the fault tolerance of the model.

3) SETTING THE TIME-POINT CONSTRAINTS FOR THE PD PROPOSITIONS

If the alarm of the i^{th} PD is received with a timestamp of t_i, then the time-point constraint of corresponding proposition is specified to be $[t_i, t_i]$ for temporal reasoning. Otherwise, it will be specified as $\emptyset$.

D. MATRIX REASONING ALGORITHM

The reasoning algorithm of TCFPNs is based on interval operations and matrix operations. Prior to describing the reasoning algorithm, some functions or operators are defined as follows.

1)Null function $N(\ )$:

$$\boldsymbol{A} = N(\boldsymbol{T}^{\mathrm{a}}) \Leftrightarrow A_{ij} = \begin{cases} 1, & T^a_{ij} \neq \emptyset \\ 0, & T^a_{ij} = \emptyset \end{cases} \tag{3}$$

where $\boldsymbol{A}$ is $(m \times n)$-dimensional real matrix and $\boldsymbol{T}^{\mathrm{a}}$ is $(m \times n)$-dimensional time interval matrix.

2)Match function $M(\ )$:

$$\boldsymbol{A} = M(\boldsymbol{T}^{\mathrm{a}}, \boldsymbol{T}^{\mathrm{b}}) \Leftrightarrow A_{ij} = \begin{cases} 1, & T^a_{ij} \subseteq T^b_{ij} \\ 0, & T^a_{ij} \not\subset T^b_{ij} \end{cases} \tag{4}$$

where $\boldsymbol{A}$ is $(m \times n)$-dimensional real matrix,$\boldsymbol{T}^{\mathrm{a}}$ and $\boldsymbol{T}^{\mathrm{b}}$ are $(m \times n)$-dimensional time interval matrices.

3)Intersect multiplication operator $\hat{\times}$:

$$\boldsymbol{T}^{\mathrm{b}} = \boldsymbol{T}^{\mathrm{a}} \ \hat{\times}\ \boldsymbol{B} \Leftrightarrow T^b_{ij} = \bigcap_{1\le g\le n, B_{gj}\neq 0} T^a_{ig} \tag{5}$$

where $\boldsymbol{T}^{\mathrm{a}}$ and $\boldsymbol{T}^{\mathrm{b}}$ are $(m \times n)$ and $(m \times k)$-dimensional interval matrices, and $\boldsymbol{B}$ is $(n\times k)$-dimensional logical matrix.

4)Interval merge operator $\oplus$:

$$\boldsymbol{T}^{\mathrm{c}} = \boldsymbol{T}^{\mathrm{a}} \oplus \boldsymbol{T}^{\mathrm{b}} \Leftrightarrow Tc_{ij} = \begin{cases} T^a_{ij}, & \text{if } T^a_{ij} \neq \emptyset \text{and} T^a_{ij} \subseteq T^b_{ij} \\ T^a_{ij} \cup T^b_{ij}, & \text{else} \end{cases} \tag{6}$$

where $\boldsymbol{T}^{\mathrm{a}}$, $\boldsymbol{T}^{\mathrm{b}}$, and $\boldsymbol{T}^{\mathrm{c}}$are all $(m \times n)$-dimensional interval matrices.

5)Input reasoning operator $\odot$:

$$\left\{\boldsymbol{C},\ \boldsymbol{T}^{\mathrm{c}}\right\} = \left\{\boldsymbol{A},\ \boldsymbol{T}^{\mathrm{a}}\right\} \odot \boldsymbol{B} \Leftrightarrow \begin{cases} C_{ij} = \underset{1\le g\le n, B_{gj}\neq 0}{\mathrm{avg}} A_{ig} \\ \boldsymbol{T}^{\mathrm{c}}_{ij} = \bigcap\limits_{1\le g\le n, B_{gj}\neq 0} T^a_{ig} \end{cases} \tag{7}$$

where $\boldsymbol{A}$ and $\boldsymbol{C}$ are $(m \times n)$,$(m \times k)$-dimensional real matrices, $\boldsymbol{T}^{\mathrm{a}}$ and $\boldsymbol{T}^{\mathrm{c}}$ are $(m \times n)$, $(m \times k)$-dimensional interval matrices, and $\boldsymbol{B}$ is $(n\times k)$-dimensional logical matrix. The ''avg'' represents the average operation of real number.

6) Output reasoning operator $\otimes$:

$$\left\{\boldsymbol{C},\boldsymbol{T}^{\mathrm{c}}\right\} = \left\{\boldsymbol{A},\ \boldsymbol{T}^{\mathrm{a}}\right\} \otimes \boldsymbol{B} \Leftrightarrow \begin{cases} C_{ij} = \underset{1\le g\le n, B_{gj}\neq 0}{\max} A_{ig} \\ \boldsymbol{T}^{\mathrm{c}}_{ij} = T^a_{ig}\left|_{1\le g\le n \text{ and } A_{ig}=C_{ij}}\right. \end{cases} \tag{8}$$

where $\boldsymbol{A}$ and $\boldsymbol{C}$ are $(m \times n)$,$(m \times k)$- dimensional real matrices, $\boldsymbol{T}^{\mathrm{a}}$ and $\boldsymbol{T}^{\mathrm{c}}$ are $(m\times n)$, $(m\times k)$-dimensional interval matrices, and $\boldsymbol{B}$ is -dimensional logical matrix.

Based on the defined operators and the hierarchical structure of diagnosis model, the reasoning algorithm of TCFPNs can be performed by the following five steps.

1) The input and output reasoning of layer 3:

$$\left\{\boldsymbol{\theta}_{\boldsymbol{P}3}{}', \boldsymbol{T}_{\boldsymbol{P}3}{}'\right\} = \left(\left\{\boldsymbol{\theta}_{\boldsymbol{P}4}, \boldsymbol{T}_{\boldsymbol{P}4} - \boldsymbol{D}_{\boldsymbol{R}3} \hat{\times} \boldsymbol{I}_3^T\right\} \odot \boldsymbol{I}_3\right) \otimes \boldsymbol{O}_3^T \tag{9}$$

where $\boldsymbol{\theta}_{\boldsymbol{P}4}$ and $\boldsymbol{T}_{\boldsymbol{P}4}$ represent the truth degree and the time-point constraint vectors for the propositions in group $\boldsymbol{P}_4$, and $\boldsymbol{D}_{\boldsymbol{R}3}$ is the time-distance constraint vector for the rules in group $\boldsymbol{R}_3$. These parameters can be determined in the parameter setting section. Besides, $\boldsymbol{\theta}_{\boldsymbol{P}3}{}'$ and $\boldsymbol{T}_{\boldsymbol{P}3}{}'$ are temporary variables for the propositions in group $\boldsymbol{P}_3$, which represent the output of the layer 3 of the model.

2) Update the fault information of the propositions in $\boldsymbol{P}_3$:

$$\begin{cases} \boldsymbol{\theta}_{\boldsymbol{P}3} = \left(\boldsymbol{\theta}_{\boldsymbol{P}3} + \boldsymbol{\theta}'_{\boldsymbol{P}3} + M\left(\boldsymbol{T}_{\boldsymbol{P}3}, \boldsymbol{T}'_{\boldsymbol{P}3}\right)\right)/3 \\ \boldsymbol{T}_{\boldsymbol{P}3} = \boldsymbol{T}_{\boldsymbol{P}3} \oplus \boldsymbol{T}'_{\boldsymbol{P}3} \end{cases} \tag{10}$$

In this step, the information of the PR propositions and the CB propositions are initially integrated.

3) The input and output reasoning of the layer 2:

$$\{\boldsymbol{\theta}_{\boldsymbol{P}2}, \boldsymbol{T}_{\boldsymbol{P}2}\} = \left(\left\{\boldsymbol{\theta}_{\boldsymbol{P}3}, \boldsymbol{T}_{\boldsymbol{P}3} - \boldsymbol{D}_{\boldsymbol{R}2} \hat{\times} \boldsymbol{I}_2^T\right\} \odot \boldsymbol{I}_2\right) \otimes \boldsymbol{O}_2^T \tag{11}$$

4) The input and output reasoning of the layer 1:

$$\{\boldsymbol{\theta}_{\boldsymbol{P}1}, \boldsymbol{T}_{\boldsymbol{P}1}\} = \left(\left\{\boldsymbol{\theta}_{\boldsymbol{P}2}, \boldsymbol{T}_{\boldsymbol{P}2} - \boldsymbol{D}_{\boldsymbol{R}1} \hat{\times} \boldsymbol{I}_1^T\right\} \odot \boldsymbol{I}_1\right) \otimes \boldsymbol{O}_1^T \tag{12}$$

5) Update the truth degree of the proposition in $\boldsymbol{P}_1$:

$$\boldsymbol{\theta}_{\boldsymbol{P}1} = \left(\boldsymbol{\theta}_{\boldsymbol{P}1} + N\left(\boldsymbol{T}_{\boldsymbol{P}1}\right)\right)/2 \tag{13}$$

After a round of reasoning, the truth degree and time-point constraint of the proposition in $\boldsymbol{P}_1$ can be obtained, which represent the diagnosis results for the corresponding section.

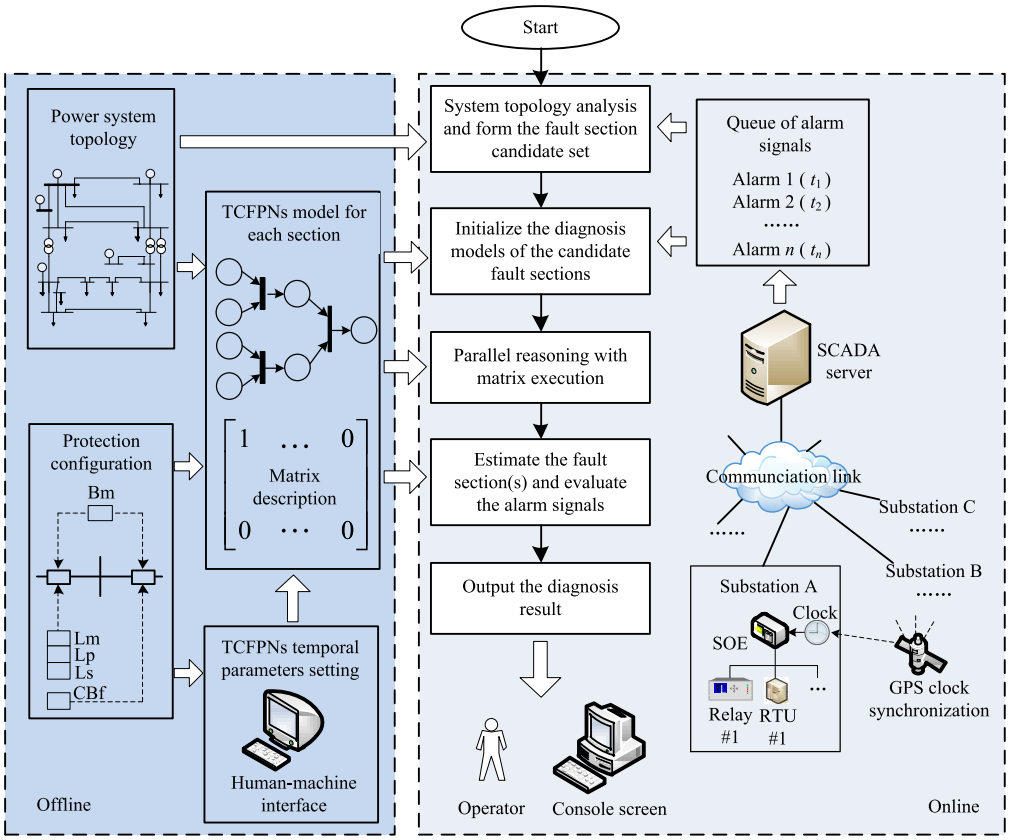

FIGURE 6. The framework of the TCFPNs based power system fault diagnosis.

The section with a truth degree higher than a certain threshold will be determined as the fault section, and in this paper, the threshold value is taken as 0.6, which is proved to be appropriate by plenty of case studies.

IV. THE FRAMEWORK OF THE TCFPNs BASED POWER SYSTEM FAULT DIAGNOSIS

The framework of the TCFPNs based method for power system fault diagnosis is shown in Fig. 6. First, the outage area can be determined by topological analysis using the CB alarms [30]. Thereafter, the diagnosis models of the candidate sections in the outage area are initialized based on the real-time alarms queue obtained from the SCADA system. Through the parallel matrix reasoning process, the truth degree of each section as well as its time-point constraint can be obtained. Besides, the operating performance for the PDs can be evaluated according to the reasoning results. Finally, the critical information is sent to the operator for decision-making. Noted that the diagnosis models are established offline, and therefore it will not affect the performance of the real-time fault diagnosis.

Besides, although the above analysis is described for ordinary wiring system, it is actually suitable for power systems with double-bus or 3/2 wiring systems. Taking the 3/2 wiring system as an example, since this wiring mode is usually used for the 500kV power grid in China, the system has higher requirements for stability, and needs to remove of the fault as fast as possible (usually within 100ms). Therefore, in addition to the aforementioned primary backup protection and secondary backup protection, it is necessary to consider the configuration of breaker failure protection and dead zone protection. Under this background, the proposed method only needs to adjust the diagnostic model based on the protection configuration of the system, and there is no need to adjust the matrix algorithm. Related studies can be found in [31]. Therefore, the proposed method has good versatility and can be applied to power grids with different structures.

V. CASE STUDIES

A. TEST SYSTEM #1

In order to verify the effectiveness of the TCFPNs based method, a large number of scenarios are tested for the IEEE 14-bus power system as shown in Fig. 1, and some of the testing results are shown in the Table 2.

In Table 2, cases 1-3 are scenarios with the complete alarms, and cases 4-7 are scenarios under complex conditions with the false timestamp, error alarm or missing alarm. Among them, the case 6 and 7 are the diagnosis of multiple fault scenarios. Due to the space limitation, only the detailed reasoning process of case 1 is given as follows.

According to the alarms and the diagnosis model of B13 (shown in fig. 3), the information of the propositions in group

TABLE 2. Testing results for the IEEE 14-bus power system scenarios.

No.	Alarms queue $\{A_i(t_i/\text{ms})\}$	Candidate sections	Reasoning result using the TCFPNs			Truth degree of [28, 29]
			Truth degree	Time-point constraint /ms	Performance Evaluation	
1	L1213s(0), L0613s(7), L1413s(9), CB1213(54), CB0613(58), CB1413(60)	**B13** L0613 L1213 L1314	**0.9417** 0.3125 0.3125 0.3125	[-2091, -1900] ∅ ∅ ∅	B13m→RO	0.665 0.3955 0.3955 0.3955
2	L1314m(0), L1413m(2), CB1413(51), CB1314f(210), CB1212(265), CB1306(268)	**L1314** B13	**0.9667** 0.2056	[-10, -8] ∅	CB1314→RO	0.8645 0.45
3	B13m(0), CB1312(48), CB1306(51), L1213p(200), CB1213(252), L1413s(1989), CB1413(2041)	**B13** L1213 L1314	**0.9639** 0.3521 0.1833	[-20, -10] ∅ ∅	L1213p→MO CB1314→RO	0.7917 0.443 0.263
4	L1314m(0), CB1314(48), L1413p(545), CB1413(545)	**L1314**	**0.8792**	[-20, -10]	L1413m→RO L1413p→FT	0.702
5	L1314m(0), L1413m(2), CB1413(51), CB1314(55), CB1413f(210), CB1409(265)	**L1314** B14	**0.975** 0.2	[-18, -10] ∅	CB1413f→MO	0.8483 0.3555
6	L1314m(0), B13m(30), CB1314(48), CB1413(50), CB1312(81), CB1306(82)	**L1314** **B13**	**0.8292** **0.9194**	[-20, -10] [10, 20]	L1803m→MA	0.72 0.702
7	B13m(0), CB1312(48), CB1306(51), L1314m(200), B07m(250), CB0708(301), CB0704(302), L1413s(1989), CB1413(2041)	**B13** **B07** L1314	**0.9639** **0.8806** 0.1875	[-20, -10] [230, 240] ∅	CB1314→RO L1314m→EA CB0709→MA	0.7917 0.72 0.288

Notes: RO means that the PD refuse to operate; MO represents the mal-operation of PD; FT represents the alarm has a false timestamp; MA represents the missing alarm of PD; and EA represents the error alarm of PD.

$\boldsymbol{P}_4$ and $\boldsymbol{P}_3$ can be initialized as

$$\begin{cases} \boldsymbol{\theta}_{\boldsymbol{P}4} = [0.2, 0.9, 0.2, 0.9, 0.2, 0.9] \\ \boldsymbol{T}_{\boldsymbol{P}4} = [\emptyset, [58,58], \emptyset, [54,54], \emptyset, [60,60]] \\ \boldsymbol{\theta}_{\boldsymbol{P}3} = [0.4, 0.75, 0.4, 0.75, 0.4, 0.75] \\ \boldsymbol{T}_{\boldsymbol{P}3} = [\emptyset, [7,7], \emptyset, [0,0], \emptyset, [9,9]] \end{cases}$$

Then the first reasoning step will result in

$$\begin{cases} \boldsymbol{\theta}_{\boldsymbol{P}3}' = [0.2, 0.9, 0.2, 0.9, 0.2, 0.9] \\ \boldsymbol{T}_{\boldsymbol{P}3}' = [\emptyset, [-2,18], \emptyset, [-6,-14], \emptyset, [0,20]] \end{cases}$$

The second reasoning step will result in

$$\begin{cases} \boldsymbol{\theta}_{\boldsymbol{P}3} = [0.2, 0.883, 0.2, 0.883, 0.2, 0.883] \\ \boldsymbol{T}_{\boldsymbol{P}3} = [\emptyset, [7,7], \emptyset, [0,0], \emptyset, [9,9]] \end{cases}$$

The third reasoning step will result in

$$\begin{cases} \boldsymbol{\theta}_{\boldsymbol{P}2} = [0.883, 0.883, 0.883] \\ \boldsymbol{T}_{\boldsymbol{P}2} = [[-2093,-1893], [-2100,-1900], [-2091,-1891]] \end{cases}$$

The forth reasoning step will result in

$$\begin{cases} \boldsymbol{\theta}_{\boldsymbol{P}1} = [0.883] \\ \boldsymbol{T}_{\boldsymbol{P}1} = [[-2091,-1900]] \end{cases}$$

The final reasoning step will result in

$$\boldsymbol{\theta}_{\boldsymbol{P}1} = [0.9417]$$

Since the obtained truth degree is larger than 0.6, B13 is determined as a fault section, and the time-point constraints of the fault occurrence is $[-2091, -1900]$ ms. Similarly, the truth degrees for other candidate sections are reasoned to be 0.3125, which indicates that L0613, L1213 and L1314 are not the fault sections. According to the actual fault section, it can be easily judged that B13m refuses to operate in the fault removing process.

The reasoning processes of the other cases are similar. According to the results shown in the Table 2, the proposed method is capable of diagnosing the fault section for single-fault as well as multi-fault conditions, even when the scenarios are with abnormal operations or error alarms of the PDs. The missing alarm or false timestamp will reduce the truth degree of the fault section, and the error alarm will increase the truth degree of normal section, but they will not affect the final result of fault section estimation. Comparing with the method presented in [28], [29], the fault tolerance of the model can be improved significantly, since the fault section has a higher confidence degree while the normal section has a lower confidence degree.

B. TEST SYSTEM #2

To further verify the practicability of the proposed method, an actual fault scenario happened at Zhejiang provincial power system in China is tested here [10]. The related part

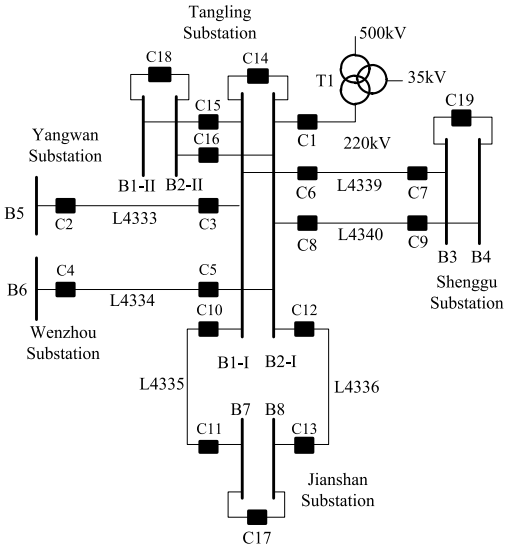

FIGURE 7. Power network associated with the fault scenario.

TABLE 3. The received alarms.

Substation	Queue of alarms	Time(ms)
Tangling	MPR of L4335 operates	0
Jianshan	MPR of L4335 operates	5
Jianshan	MPR of L4336 operates	30
Jianshan	C11 is tripped off	52
Tangling	C12 is tripped off	78
Jianshan	C13 is tripped off	84
Tangling	C10 is tripped off	160
Tangling	BFPR of C10 operates	203
Tangling	C3 is tripped off	249
Tangling	C14 is tripped off	249
Tangling	C6 is tripped off	250
Tangling	C15 is tripped off	253
Tangling	MPR of B2-I operates	340
Tangling	C1 is tripped off	389
Tangling	C5 is tripped off	390
Tangling	C8 is tripped off	390
Tangling	C16 is tripped off	390

of the 220kV power grid and the received alarms are shown in Fig. 7 and Table 3, where the timestamp of the first alarm is taken as the time reference.

According to the received alarms, the set of candidate sections in the outage area can be determined as {L4335, L4336, B1-I, B2-I}. Through the parallel matrix reasoning of each diagnosis model for the candidate section, the diagnosing result and performance evaluation of the PDs are shown in the Table 4.

Referring to the recorded data, the actual fault scenario was checked out that the first fault occurred on L4335 first at -13ms, another fault occurred on L4336 at 17ms, and the third fault occurred on B2-I at 327ms (under the same time reference). Evidently, the actual fault sections are completely consistent with the diagnosis result, and the time point at which the fault occurs also satisfies the time point constraints obtained by reasoning algorithm.

TABLE 4. Diagnosis report of the fault scenario.

The diagnosis report	
Fault section(s)	• L4335 (during [-15,-5] ms with a truth degree of 0.9667). • L4336 (during [10,20] ms with a truth degree of 0.8291). • B2-I (during [320,330] ms with a truth degree of 0.9194).
Non-fault section(s)	• B1-I (with a truth degree of 0.2166). • B1-II (with a truth degree of 0.1583). • B2-II (with a truth degree of 0.1583).
Performance evaluation	• C10 in Tangling substation failed to trip off. • MPR of L4336 in Tangling substation operated, but the alarm was missing. • The tripping of C10 is an error alarm.
Detailed report	• A fault occurred on L4335 during [-15, -5] ms, the MPRs of L4335 at both ends operated, and C11 tripped off while C10 failed. Then the BFP of C10 operated and tripped off C3, C6, C14 and C15. • A fault occurred on L4336 during [10, 20] ms, the MPRs of L4336 on both ends operated and tripped off C12 and C13. • A fault occurred on B2-I during [320, 330] ms, the MPR of B2-I operated and tripped off C1, C5, C8 and C16.

C. PERFORMANCE ANALYSIS

Different with the existing FPNs-based methods, the TCFPNs-based method employs a layer-by-layer reasoning algorithm, and only the related partitions of the input and output matrix are involved in the reasoning of each layer. As a result, the dimension of the matrix operations can be decreased significantly. Besides, the reasoning of the temporal constraints and the truth degrees are performed simultaneously and affect each other, the diagnosing accuracy of the model is greatly improved.

To compare the calculation complexity of the algorithm in terms of temporal reasoning, assume that m is the number of the received alarms, and k is the number of suspected faulty sections. The method proposed in [23] needs to search all possible fault sections for each received alarm, and then diagnosis each candidate section using all related alarms. The calculation complexity for temporal reasoning is $O(m^3k)$. As for the method in [28], the timing constraint relationship needs to be determined by searching the associated index table, and the calculation complexity is $O(2^mk)$. The method proposed in [32] needs to cross-check the timing constraints of the alarm information on both sides of the Petri nets model, and the calculation complexity is $O(\mathrm{m}^2\mathrm{k})$. In contrast, if the proposed matrix reasoning algorithm is used, the temporal reasoning process is embedded into the fuzzy reasoning, and the calculation complexity is $O(mk)$.

TABLE 5. Comparisons with the existing methods.

Method in	This paper	[12]	[18]	[26]	[28, 29]
Temporal information	Yes	No	No	Yes	Yes
Uncertainty considering	Yes	No	Yes	No	Yes
Diagnosis model	TCFPNs	DPNs	FPNs	TCN	TCN+ FPNs
Structure optimization	Yes	Yes	Yes	No	No
Inference efficiency	High	High	High	Low	Medium
Fault Tolerance	Strong	Low	Low	Medium	Strong

Therefore, the method proposed in this paper has better computational efficiency.

All the cases tested in this paper are implemented in a PC with 2.3GHz dual-core processor (Intel Core i3-2350M) and 2G memory using MATLAB programming, and the diagnosis time is within 5ms, which indicates that the proposed method totally meets online requirements.

The comparisons between the proposed method and other existing methods are given in Table 5.

Since the truth degree and the timing contribute of the alarms are introduced into the TCFPNs, the uncertainty and the temporal information of the alarms can be fully utilized. Besides, the structure of the graphic model is further optimized based on the protection configuration of the system, the adaptability of the method is enhanced. All the fuzzy reasoning and temporal reasoning calculations are performed by the layer-by-layer matrix reasoning algorithm, the inference efficiency is very high. Besides, since the temporal reasoning result is considered to influence the fuzzy reasoning process, the fault tolerance of the proposed method is relatively strong. Compared with other method in Tab 5, the real fault section has a higher confidence degree while the normal section has a lower confidence degree.

VI. CONCLUSION

The timestamp information of the alarms contains a wealth of information for power system fault diagnosis. In this paper, a novel TCFPNs based method is proposed for power system fault diagnosis. Firstly, the mathematical model of the TCFPNs is defined based on the advantages of existing FPNs and TCN, and the uncertainty and the temporal information of the alarms can be considered by the graphic model. Based on the graphic model, the matrix description of the TCFPNs is constructed, and the layer-by-layer parallel matrix reasoning algorithm is then carried out to obtain the truth degree as well as the time point constraint of the fault section simultaneously. Finally, different power systems are selected to perform the case studies and the testing results demonstrate the feasibility, efficiency and fault tolerance of the method. Future efforts will be made in online structuring of the TCFPNs, thereby further improving its adaptability and engineering practicality.

REFERENCES

[1] E. V. M., O. L. C. M., and H. J. A. F., "An on-line expert system for fault section diagnosis in power systems," *IEEE Trans. Power Syst.*, vol. 12, no. 1, pp. 357–362, Feb. 1997.

[2] H.-J. Lee, D.-Y. Park, B.-S. Ahn, Y.-M. Park, J.-K. Park, and S. S. Venkata, "A fuzzy expert system for the integrated fault diagnosis," *IEEE Trans. Power Del.*, vol. 15, no. 2, pp. 833–838, Apr. 2000.

[3] T. Bi, F. Wen, Y. Ni, and F. F. Wu, "Distributed fault section estimation system using radial basis function neural network and its companion fuzzy system," *Int. J. Elect. Power Energy Syst.*, vol. 25, no. 5, pp. 377–386, Jun. 2003.

[4] G. Xiong, D. Shi, J. Chen, L. Zhu, and X. Duan, "Divisional fault diagnosis of large-scale power systems based on radial basis function neural network and fuzzy integral," *Electr. Power Syst. Res.*, vol. 105, pp. 9–19, Dec. 2013.

[5] Z. Yongli, H. Limin, and L. Jinling, "Bayesian networks-based approach for power systems fault diagnosis," *IEEE Trans. Power Del.*, vol. 21, no. 2, pp. 634–639, Apr. 2006.

[6] S. Lin, X. Chen, and Q. Wang, "Fault diagnosis model based on Bayesian network considering information uncertainty and its application in traction power supply system," *IEEJ. Trans. Electr. Electron. Eng.*, vol. 13, no. 5, pp. 671–680, Jan. 2018.

[7] W.-H. Chen, "Online fault diagnosis for power transmission networks using fuzzy digraph models," *IEEE Trans. Power Del.*, vol. 27, no. 2, pp. 688–698, Apr. 2012.

[8] S.-W. Min, J.-M. Sohn, J.-K. Park, and K.-H. Kim, "Adaptive fault section estimation using matrix representation with fuzzy relations," *IEEE Trans. Power Syst.*, vol. 19, no. 2, pp. 842–848, May 2004.

[9] W. Guo, F. Wen, G. Ledwich, Z. Liao, X. He, and J. Liang, "An analytic model for fault diagnosis in power systems considering malfunctions of protective relays and circuit breakers," *IEEE Trans. Power Del.*, vol. 25, no. 3, pp. 1393–1401, Jul. 2010.

[10] Y. Zhang, C. Y. Chung, F. Wen, and J. Zhong, "An analytic model for fault diagnosis in power systems utilizing redundancy and temporal information of alarm messages," *IEEE Trans. Power Syst.*, vol. 31, no. 6, pp. 4877–4886, Nov. 2016.

[11] K. L. Lo, H. S. Ng, and J. Trecat, "Power systems fault diagnosis using Petri nets," *IEE Proc.-Gener., Transmiss. Distrib.*, vol. 144, no. 3, pp. 231–236, May 1997.

[12] M. T. Yousef, A. A. El Fergany, and A. A. El Alaily, "Fault diagnosis of power systems using binary information of breakers and relays through DPNs," in *Proc. Int. Conf. Power Syst. Technol.*, Oct. 2002, pp. 1122–1126.

[13] M. Gao, M. Zhou, X. Huang, and Z. Wu, "Fuzzy reasoning Petri nets," *IEEE Trans. Syst., Man, Cybern. A, Syst. Humans*, vol. 33, no. 3, pp. 314–324, May 2003.

[14] H.- C. Liu, L. Liu, Q.-L. Lin, and N. Liu, "Knowledge acquisition and representation using fuzzy evidential reasoning and dynamic adaptive fuzzy Petri nets," *IEEE Trans. Cybern.*, vol. 43, no. 3, pp. 1059–1072, Jun. 2013.

[15] X. Zhang and S. Yao, "Fuzzy stochastic Petri nets and analysis of the reliability of multi-state systems," *IET Softw.*, vol. 9, no. 3, pp. 83–93, Jun. 2015 .

[16] H. Zhang, "Fault diagnosis system of wind turbine generator based on Petri net," *Appl. Mech., Mechatron. Intell. Syst. (AMMIS)*, 2016, pp. 311–318.

[17] J. Sun, S.-Y. Qin, and Y.-H. Song, "Fault diagnosis of electric power systems based on fuzzy Petri nets," *IEEE Trans. Power Syst.*, vol. 19, no. 4, pp. 2053–2059, Nov. 2004.

[18] X. Luo and M. Kezunovic, "Implementing fuzzy reasoning Petri-nets for fault section estimation," *IEEE Trans. Power Del.*, vol. 23, no. 2, pp. 676–685, Apr. 2008.

[19] Z. Y. He, J. W. Yang, Q. F. Zeng, and T. L. Zang, "Fault section estimation for power systems based on adaptive fuzzy Petri nets," *Int. J. Comput. Intell. Syst.*, vol. 7, no. 4, pp. 605–614, Jul. 2014.

[20] X. Zhang, S. Yue, and X. Zha, "Method of power grid fault diagnosis using intuitionistic fuzzy Petri nets," *IET Gener. Transmiss. Distrib.*, vol. 12, no. 2, pp. 295–302, Jan. 2018.

[21] Z. A. Vale and A. M. E. Moura, "An expert system with temporal reasoning for alarm processing in power system control centers," *IEEE Trans. Power Syst.*, vol. 8, no. 3, pp. 1307–1314, Aug. 1993.
[22] Y.-C. Huang, H.-T. Yang, and C.-L. Huang, "A new intelligent hierarchical fault diagnosis system," *IEEE Trans. Power Syst.*, vol. 12, no. 1, pp. 349–356, Feb. 1997.
[23] W. Guo, F. Wen, G. Ledwich, Z. Liao, X. He, and J. Huang, "A new analytic approach for power system fault diagnosis employing the temporal information of alarm messages," *Int. J. Elect. Power Energy Syst.*, vol. 43, no. 1, pp. 1204–1212, Dec. 2012.
[24] R. Dechter, I. Meiri, and J. Pearl, "Temporal constraint networks," *Artif. Intell.*, vol. 49, nos. 1–3, pp. 61–95, May 1991.
[25] W. Guo, F. Wen, Z. Liao, L. Wei, and J. Xin, "An analytic model-based approach for power system alarm processing employing temporal constraint network," *IEEE Trans. Power Del.*, vol. 25, no. 4, pp. 2435–2447, Oct. 2010.
[26] Y. Cui, J. Shi, and Z. Wang, "Power system fault reasoning and diagnosis based on the improved temporal constraint network," *IEEE Trans. Power Del.*, vol. 31, no. 3, pp. 946–954, Jun. 2016.
[27] T.-F. Kang, W. Wu, B.-M. Zhang, P. Li, and W.-F. Zhang, "Temporal abductive reasoning based diagnosis and alarm for power grid," *Proc. Chin. Soc. Elect. Eng.*, vol. 30, no. 19, pp. 84–90, Jul. 2010.
[28] Y. Zhang, F. Wen, and J. Li, "Power system fault diagnosis with an enhanced fuzzy Petri net accommodating temporal constraints," *Automat. Electr. Power Syst.*, vol. 38, no. 5, pp. 66–72, Mar. 2014.
[29] Y. Zhang, Y. Zhang, X. Zhang, F. Wen, C. Y. Chung, C.-L. Tseng, F. Zeng, and Y. Yuan, "A fuzzy Petri net based approach for fault diagnosis in power systems considering temporal constraints," *Int. J. Elect. Power Energy Syst.*, vol. 78, pp. 215–224, Jun. 2016.
[30] Y. Zhu, Y. Yang, and W. Zhang, "New methods used in a computer aided restoration system for realtime electric network topology determination & overloads correction," *Chin. Soc. Elect. Eng.*, vol. 14, no. 3, pp. 52–58, 1994.
[31] W. Yang, Y. Q. Liu, X. Z. Wu, X. G. Yin, B. Xu, X. Hao, and X. S. Li, "A fault diagnosis method of 3/2 connection substation based on Petri nets with dead-zone fault taken into account," *Power Syst. Protection Control*, vol. 45, no. 20, pp. 28–37, 2017.
[32] X. Tong, H. Xie, and M. Sun, "Power system fault diagnosis model based on layered fuzzy Petri net considering temporal constraint checking," *Automat. Electr. Power Syst.*, vol. 37, no. 6, pp. 63–68, Mar. 2013.

BIAO XU was born in Jiangxi, China, in 1993. He received the B.S. degree from the Huazhong University of Science and Technology (HUST), Wuhan, China, where he is currently pursuing the Ph.D. degree. His research interests include protective relaying and fault diagnosis of power systems.

XIN YIN (M'16) received the B.Eng. degree in electronic engineering from the University of Sheffield, U.K., in 2008, the M.Sc. degree in telecommunication from the University College London, U.K., in 2009, and the Ph.D. degree in electrical and electronic engineering from the University of Manchester, U.K., in 2016. He is currently a Postdoctoral Research Associate of electrical engineering with the University of Liverpool. His current research interests include distribution system and control of micro grid with renewable energy.

XIANGGEN YIN (M'08) received the B.S., M.S., and Ph.D. degrees in electrical engineering from the Huazhong University of Science and Technology (HUST), Wuhan, China, in 1982, 1985, and 1989, respectively, where he is currently a Professor with the School of Electrical and Electronic Engineering. His research interests include fault location, protective relaying, and power system stability control.

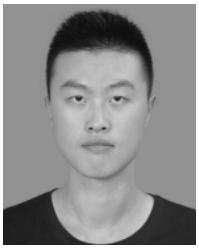

YIKAI WANG was born in Liaoning, China, in 1996. He is currently pursuing the Ph.D. degree with the Huazhong University of Science and Technology (HUST), Wuhan, China. His research interest includes protective relaying of power grid.

SHUAI PANG was born in Jiangsu, China, in 1992. He is currently pursuing the master's degree with the Huazhong University of Science and Technology (HUST), Wuhan, China. His research interest includes protective relaying of power grid.